Magnetic proximity effect at the molecular scale: First-principles calculations

Dongping Liu,[1] Yibin Hu,[2] Hong Guo,[2] and X. F. Han[1]
[1]*State Key Laboratory of Magnetism, Beijing National Laboratory for Condensed Matter Physics, Institute of Physics, Chinese Academy of Sciences, Beijing 100080, China*
[2]*Department of Physics and Center for the Physics of Materials, McGill University, Montreal, Quebec, Canada H3A 2T8*
(Received 12 October 2008; published 17 November 2008)

We report first-principles analysis of equilibrium and nonequilibrium quantum transport in a Langmuir-Blodgett (LB) film contacted by Fe electrodes. For several LB molecules with different lengths, transport is in the tunneling regime. We found that spin-polarized transport is closely related to a magnetic proximity effect that causes the LB film to develop small but finite magnetic character that determines spin-polarized current and produces unusual tunnel magnetoresistance (TMR) ratio versus bias voltage. This unusual TMR was observed experimentally.

DOI: 10.1103/PhysRevB.78.193307 PACS number(s): 85.35.−p, 72.25.Mk, 85.65.+h

Molecules have certain advantages for spin-dependent quantum transport due to relatively weak spin-orbital coupling and hyperfine interaction such that spin coherence can be maintained for longer length scales.[1] Considerable experimental[1–6] and theoretical[7–14] effort have therefore been devoted to the understanding of molecular spintronics. For magnetic tunnel junctions (MTJs) where two ferromagnetic leads sandwich a molecular layer, substantial tunneling magnetoresistance (TMR) ratios have been observed in carbon nanotubes,[2] organic semiconductors,[5] molecular wires,[4] and Langmuir-Blodgett (LB) films.[6] These hybrid ferromagnet-molecular systems showed very rich quantum transport properties by harnessing both spin and charge of the electron as well as the chemistry and material of the device. Theoretically, spin transport in molecular MTJs can be understood from a resonance transmission point of view where the resonance is sensitively dependent on the relative orientation of the magnetic moments in the ferromagnetic leads.[11] From another point of view, wave-function symmetry matching at the ferromagnetic or molecule interface can critically affect spin-polarized conduction.[14] While these physical mechanisms provide a good level of understanding, there is an important aspect that has not been carefully investigated before, namely, the *molecular scale* magnetic proximity effect.

When two different materials are brought into close proximity, the property of one material can transfer to the other material through electron-electron interactions. Such a proximity effect is well known in superconductor–normal material interfaces. Similarly, when a magnetic material is in touch with a nonmagnetic one, the latter can acquire some (albeit small) magnetic properties. Indeed, it was reported that carbon nanotubes can become magnetic when contacted by magnetic metal.[15] For molecular scale MTJs, we expect the proximity effect to play an important role in quantum transport properties.

Here we report first-principles theoretical investigations of the molecular scale magnetic proximity effect in the contest of molecular spintronics. To carry out the first-principles analysis, we consider a MTJ where the tunnel barrier is a LB film made of π-conjugated pyrrole derivative 3-hexadecyl pyrrole [3HDP, Fig. 1(a)]. Figure 1(c) plots the *scattering region* of the MTJ which consists of the LB film sandwiched by three Fe buffer layers; the scattering region is connected to the left or right Fe leads [not shown in Fig. 1(c)]. The Fe layers are oriented in the (001) direction. An advantage of LB films is that they can be easily prepared experimentally on large wafers. Experimentally, these LB films exhibit relatively large TMR of ~20% and stable switching ability at room temperature.[6] In our analysis, the length of the carbon chain attached to the 3HDP ring [labeled R in Fig. 1(a)] was varied from zero to C_8H_{17} (length ~ 10.02 Å). We name the molecule with R=0 (having only the pyrrole ring) as type I; R=2 (two CH_2 connected to the pyrrole ring) as type II; R=5 as type III; and R=8 as type IV. For all systems, the scattering region itself contains about one hundred atoms. The leads are periodic in the x-y directions and extend to $z=\pm\infty$, where bias voltage is applied and transport current measured. The atomic structures of the scattering region are fully relaxed using total-energy density-functional theory (DFT) within the SIESTA electronic package.[16,17]

Our quantum transport calculation is based on a state-of-the-art first-principles method where real-space DFT is carried out within the Keldysh nonequilibrium Green's function (NEGF) formalism.[12,18] The basic idea of the NEGF-DFT formalism is to calculate the device Hamiltonian and electronic structure by DFT, deal with the nonequilibrium quantum transport conditions by NEGF, and account for the open device boundary conditions by the real-space numerical procedure. We refer interested readers to Refs. 12 and 18 for

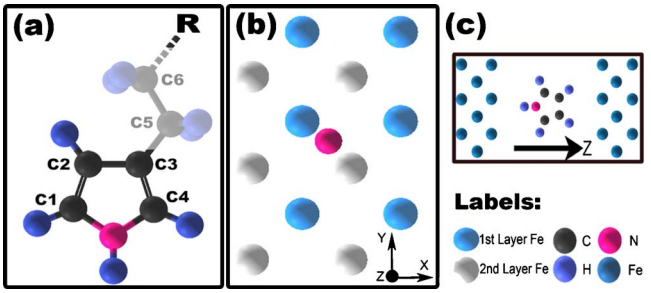

FIG. 1. (Color online) (a) 3HDP molecules in the MTJ where R is the side CH_2 chain. (b) Surface contact position of the 3HDP where nitrogen is used to indicate the bridge site (Ref. 17). The pyrrole ring plane is parallel to the y direction. (c) The scattering region of the two-probe MTJ.

 ©2008 The American Physical Society

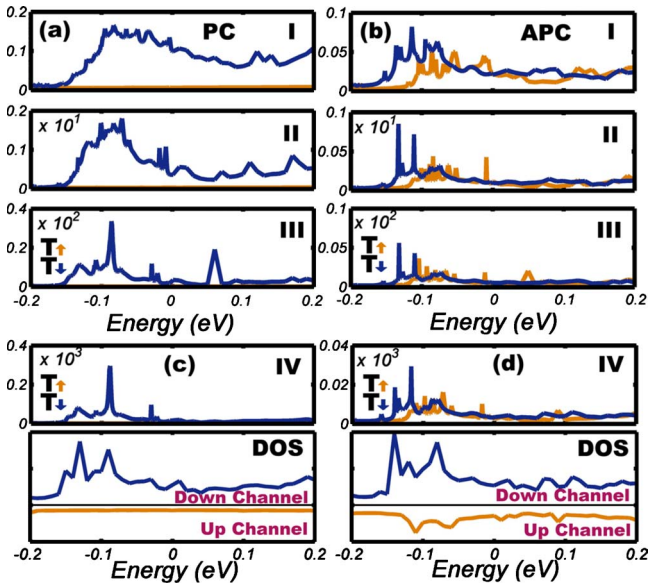

FIG. 2. (Color online) (a),(b) Transmission coefficients of types I–III systems at zero bias versus energy E in steps of 1 meV, for PC and APC, respectively. Darker (blue) lines are for spin-down channel and lighter (orange) lines are for spin-up channel. (c) and (d) are data for type IV system. Upper panels are transmission and lower panels are total density of states of the molecule. All PC spin-up transmission coefficients are very small and the lighter lines almost cannot be seen.

details of the NEGF-DFT formalism. After the self-consistent NEGF-DFT iteration of the device Hamiltonian is converged,[19] we calculate the spin-resolved transmission coefficient from the standard Green's function method[12] as $T_\sigma(E,V_b)=\mathrm{Tr}[\Gamma_l(E)G^R(E)\Gamma_r(E)G^A(E)]$, where E is the electron energy and V_b the external bias voltage. Quantities $G^{R,A}$ are retarded and advance Green's functions and $\Gamma_{l,r}$ are the linewidth functions of the left and right leads.[18]

Figure 2 plots spin-resolved transmission coefficients $T_\sigma(E)$ versus energy E near the Fermi level of the leads (shifted to $E_f=0$) at zero bias. For parallel configuration (PC) of the magnetic moments of the two Fe leads, only the spin-down channel $\sigma=\downarrow$ has substantial transmission and $T_\uparrow(E)\approx 0$ near E_f. For antiparallel configuration (APC), both $T_\uparrow$ and $T_\downarrow$ contribute substantially to total transmission $T=T_\uparrow+T_\downarrow$. For both PC and APC, $T_\sigma(E)$ sharply reduces when the carbon chain length R is increased from zero to eight. Since the electronic states of LB molecules are of (s,p) nature, there is no magnetism in these molecules. When contacted by ferromagnetic metal, a degree of electronic hybridization occurs which is the origin of the magnetic proximity effect that gives rise to the spin dependent transport shown in Fig. 2. To demonstrate this proximity, in Figs. 2(c) and 2(d) we plot the density of states (DOS) of the molecule inside the device and we find that the s,p-derived DOS has indeed developed spin splitting. Although the proximity-induced magnetic moment in the molecules is small, it gives substantial differences between $T_\uparrow(E)$ and $T_\downarrow(E)$, as shown in Fig. 2. Indeed, the features of the DOS and transmission coefficients are totally consistent with each other [see Figs. 2(c) and 2(d)]. In both quantities, a prominent feature is a peak structure at around $E\approx -0.1$ eV, which plays an important role for nonlinear tunnel magnetoresistance ratio (see below). When the side chain length is increased, this peak structure becomes sharper.

The proximity effect can be further identified by calculating a local projected spin-resolved DOS $D_\sigma(E)$ on each atom across the scattering region. For an isolated LB molecule, there are no magnetic moments and $D_\uparrow(E)=D_\downarrow(E)$. When the molecule is contacted by Fe, small but clear moments develop on the atoms of the molecule so that $D_\uparrow(E)\neq D_\downarrow(E)$. Figure 3 plots $\Delta D\equiv D_\uparrow-D_\downarrow$ on each carbon atom for the longest molecule (type IV). Several observations are in order. First, deep in the Fe buffer layers, $D_\uparrow>D_\downarrow$, but it is $D_\uparrow<D_\downarrow$ at the surface Fe layer which contacts the molecule. In addition, the polarization measured by the value of $|\Delta D|$ is enhanced at the surface Fe buffer layer, which is due to an energy-level shift caused by surface confinement[20] of Fe. Second, spin polarization happens on each carbon atom by proximity to the Fe atoms. In particular, $D_\uparrow<D_\downarrow$ throughout the molecule in PC [Fig. 3(a)]. For APC $D_\uparrow<D_\downarrow$ for carbon atoms near the left Fe buffer layer, while $D_\uparrow>D_\downarrow$ for those near the right Fe. Namely, the polarization on the molecule follows that of the Fe layer on either side of the molecule. In other words, for APC, the spin-up channel is largely determined by the right Fe surface and the spin-down channel by the left Fe surface. Third, we label the carbon atoms as C_n

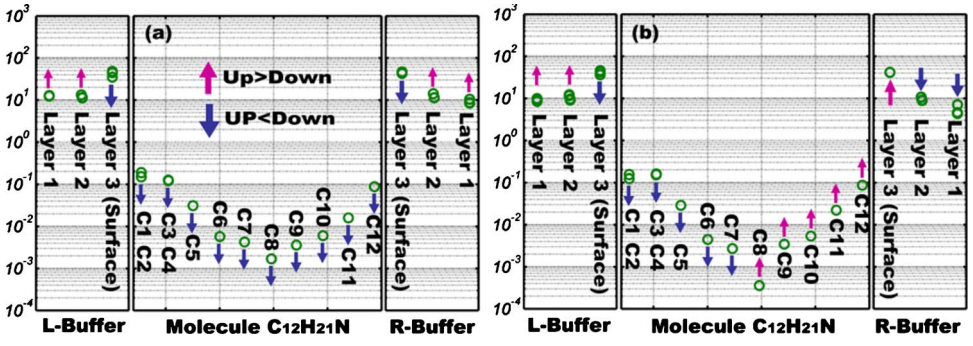

FIG. 3. (Color online) Proximity-induced magnetic character of the type IV molecule measured by $\Delta D\equiv D_\uparrow-D_\downarrow$ (green/light gray circles, vertical axis), where D_σ is the total spin-resolved density of states at Fermi level ($E_f=0$) projected on each carbon atom. The arrows indicate which D_σ is larger. (a) and (b) are for PC and APC, respectively. Side boxes labeled "L/R buffer" show ΔD of the Fe layers. Note that there is a reversal of magnetic moment in the Fe layer closest to the molecule.

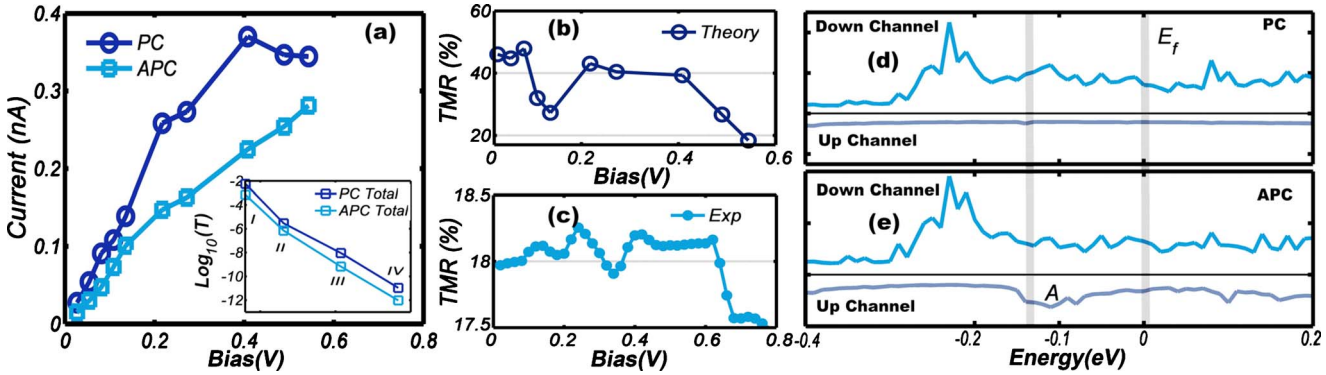

FIG. 4. (Color online) (a) *I-V* curves for type-IV device. Inset: semilog plot of $T(E_f)$ versus length for PC (higher curve) and APC (lower). (b) TMR versus bias by theory. (c) TMR versus bias measured experimentally. (d) and (e) Total DOS on the molecule at $V_b = 0.136$ V for PC and APC. The thick vertical lines indicate bias window. The letter A in (e) indicates a DOS feature that enters the bias window.

with $n=1,\ldots 4$ being those in the pyrrole ring and the rest are in the side chain R with larger n closer to the right Fe [see Fig. 1(a)]. Figure 3 shows that D_σ is much larger for those atoms closer to the Fe where the proximity effect is clearly stronger. Quantitatively, ΔD is larger for PC than in APC, as expected. Finally, comparing D_σ of each carbon atom, we find that the proximity-induced spin polarization is easier to occur in the pyrrole ring than in the side-carbon chain. These results clearly indicate that the LB molecule develops a finite magnetic character due to proximity to the Fe surfaces.

Figure 2 indicates that the total transmission coefficient T reduces drastically as R is increased. Because the Fermi level of the leads aligns in between the highest occupied molecular orbital–lowest unoccupied molecular orbital (HOMO-LUMO) gap of the molecules, we expect transport physics to be tunneling such that[21] $T \sim \exp(-\beta d)$, where d is the length of the molecule and β is an inverse of a characteristic length scale of the tunnel junction. The inset of Fig. 4(a) is a semilog plot of T at E_f versus length (labeled by the type of molecule). Indeed, the nearly linear dependence of $\log(T)$ suggests that transport is in the tunneling regime. Neglecting the data point of type I which has R=0, we found $\beta \approx 0.75$, consistent with the known result for alkanethiol molecular wires.[21] If type I data are included, a slightly larger β is obtained. This is expected because the pyrrole ring has a π electron system while the alkane chain is σ bonded; they behave differently as far as evanescent mode propagation is concerned.

The proximity-induced magnetic character in the DOS [Figs. 2(c) and 2(d)] has a substantial effect to spin-polarized current, $I_\sigma = \frac{2e}{h}\int_o^{eV_b} T_\sigma(E,V_b)(f_l - f_r)dE$, where $f_{l,r}$ are Fermi functions of the left or right leads and V_b is the bias voltage that is applied to the devices leads. When $V_b \neq 0$, qualitative features of $T_\sigma(E,V_b)$ are similar but shifted in energy to those plotted in Fig. 2 and the features in the bias window (integration window) contribute to spin-polarized current. The *I-V* curves for both PC and APC are plotted in Fig. 4(a) for the longest molecule (type IV), and $I_{PC} > I_{APC}$ as expected. From them we deduce a tunnel magnetoresistance ratio by $\mathrm{TMR} = (I_{PC} - I_{APC})/I_{PC}$. Figure 4(b) plots TMR versus V_b. The type IV device has substantial TMR values even at rather large voltage $V_b = 0.544$ V.

For these LB devices, TMR is not a simple monotonic decaying function of V_b in contrast to solid-state MTJs.[22] Tunneling is easiest when DOS features of the left and right leads align and it becomes more difficult when the alignment is broken by the bias V_b. When V_b is small, e.g., $V_b < 0.08$ V, DOS alignment has not changed substantially and transport is almost in the linear regime. As a result, TMR is roughly a constant. When V_b is increased to over 0.1 V, TMR is reduced and reaches a dip at $V_b = 0.22$ V. This reduction of TMR is due to the proximity effect as we discuss now. In Figs. 4(d) and 4(e), we plot the DOS of the molecule at $V_b = 0.136$ V for PC and APC, respectively; the two vertical lines indicate the bias window. As V_b is increased from zero, all DOS peaks shift with the profile of the voltage drop. As we discussed already (see Fig. 3), for APC the spin-up channel is largely determined by the right Fe buffer layer and the spin-down channel by the left buffer layer. Due to the asymmetry of the LB film [see Fig. 1(a)] and charge redistribution in the pyrrole ring, our calculation found that voltage drops much more on the left contact than on the right. Therefore in APC, the spin-up channel DOS shifts much slower than the increase of V_b. As a result, at $V_b = 0.136$ V the big DOS peaks in the spin-down channel for both PC and APC are shifted outside the bias window, while a spin-up DOS peak feature [indicated by letter A in Fig. 4(e)] is still in the bias window for APC, causing a relative increase of APC current, hence a decrease of TMR. Increasing V_b further, PC current increases faster than APC current due to the much greater transmission coefficient in PC (see Fig. 2). When V_b is in between ~ 0.27 and ~ 0.4 V, the DOS of both spin channels that move into the bias window is roughly independent of energy; therefore both PC and APC currents increase proportionally to each other, leading to an approximately constant TMR as shown in Fig. 4(b). Finally, TMR reduces for $V_b > 0.4$ V. We have checked that for large V_b, $T(E,V_b)$ is suppressed by V_b due to the substantial misalignment of the electronic structure of the two leads, thereby reducing the PC current and a reduction of TMR.

The first-principles transport results presented above which we found to be closely related to the molecular scale magnetic proximity effect can be compared with the experimental data in Ref. 6 collected in the laboratory of two of the

authors. First of all, the experimentally measured current[6] for LB molecules having side chain length R=16 was ~0.35 mA at bias 0.5 V, for a device having a cross section of 5×10 μm^2, giving per unit area current 7×10^{-5} nA/Å^2. Our calculated value for molecules with R=8 is 0.35 nA [see Fig. 4(a)] on a unit cell with a cross section of 49.26 Å^2. Using the scaling law of the inset of Fig. 4(a) to scale to R=16, our theoretical value of current per unit area would be 5.04×10^{-5} nA/Å^2. Although this is a very rough estimate, the order of magnitude consistency to the experimental value is assuring. Second, experimental TMR versus bias was not published in Ref. 6; it was however measured in our laboratory by scanning tunneling spectroscopy (STS) and by directly digitizing the measured *I-V* curves. Both gave exactly the same results and are plotted in Fig. 4(c) for the LB device with R=16. Since the experimental data clearly showed spin dependent tunneling, the spin-coherence length must be longer than the length of the LB molecules. The value of experimental TMR, measured at room temperature, is smaller than theoretical results. Qualitatively, the shape of the experimental TMR is also nonmonotonic, namely, there is a TMR dip followed by a flat region before further reduction by voltage. There is a uniform shift of the TMR vs bias curve by about 0.2 V in the experimental data in comparison to theory. Nevertheless, giving the many unknown experimental factors, the qualitative consistency of TMR vs bias between theory and experiment is quite reasonable and suggests that the operation of the experimental LB device[6] was dominated by the molecular scale magnetic proximity effect.

In summary, we have investigated the consequences of the molecular scale magnetic proximity effect to spin-polarized transport in the nonlinear regime. The proximity effect gives rise to a finite magnetic character to the LB molecule in terms of spin splitting of the local projected DOS. The feature of the splitting is shifted by the bias voltage, resulting in rather unusual TMR versus bias that is also seen in experimental observations. The proximity effect is strongly influenced by the molecule-metal contact, in particular by the last Fe layer. Our results strongly suggest that atomic structures of the contact layer can be used to optimize the molecular MTJ operation.

This work is supported by NSF of China (Contract No. 50721001), MOST (Contract No. 2006CB932200) (X.F.H.), NSERC of Canada, and CIFAR (H.G.).

[1] M. Ouyang and D. D. Awschalom, Science **301**, 1074 (2003); W. Harneit, C. Boehme, S. Schaefer, K. Huebener, K. Fostiropoulos, and K. Lips, Phys. Rev. Lett. **98**, 216601 (2007); S. Pramanik, C.-G. Stefanita, S. Patibandla, S. Bandyopadhyay, K. Garre, N. Harth, and M. Cahay, Nat. Nanotechnol. **2**, 216 (2007).

[2] K. Tsukagoshi, B. W. Alphenaar, and H. Ago, Nature (London) **401**, 572 (1999).

[3] V. Dediu, C. Taliani, M. Murgia, F. C. Matacotta, and S. Barbanera, Solid State Commun. **122**, 181 (2002).

[4] J. R. Petta, S. K. Slater, and D. C. Ralph, Phys. Rev. Lett. **93**, 136601 (2004).

[5] Z. H. Xiong, D. Wu, Z. V. Vardeny, and J. Shi, Nature (London) **427**, 821 (2004).

[6] T. X. Wang, H. X. Wei, Z. M. Zeng, X. F. Han, Z. M. Hong, and G. Q. Shi, Appl. Phys. Lett. **88**, 242505 (2006).

[7] H. Mehrez, J. Taylor, Hong Guo, J. Wang, and C. Roland, Phys. Rev. Lett. **84**, 2682 (2000).

[8] R. Pati, L. Senapati, P. M. Ajayan, and S. K. Nayak, Phys. Rev. B **68**, 100407(R) (2003).

[9] H. Dalgleish and G. Kirczenow, Phys. Rev. B **72**, 184407 (2005); **73**, 235436 (2006).

[10] R. Liu, S. H. Ke, H. U. Baranger, and W. T. Yang, Nano Lett. **5**, 1959 (2005).

[11] A. R. Rocha, V. M. Garcia-Suarez, S. W. Bailey, C. J. Lambert, J. Ferrer, and S. Sanvito, Nature Mater. **4**, 335 (2005).

[12] D. Waldron, Paul Haney, Brian Larade, Allan MacDonald, and Hong Guo, Phys. Rev. Lett. **96**, 166804 (2006).

[13] Bin Wang, Yu Zhu, Wei Ren, Jian Wang, and Hong Guo, Phys. Rev. B **75**, 235415 (2007).

[14] Zhannyu Ning, Yu Zhu, Jian Wang, and Hong Guo, Phys. Rev. Lett. **100**, 056803 (2008).

[15] O. Céspedes, M. S. Ferreira, S. Sanvito, M. Kociak, and J. M. D. Coey, J. Phys.: Condens. Matter **16**, L155 (2004).

[16] J. Junquera, O. Paz, D. Sanchez-Portal, and E. Artacho, Phys. Rev. B **64**, 235111 (2001).

[17] Relaxation indicates that the bridge and the hollow sites have lowest total energy. In the relaxed structure, the molecule is bonded about 3.5–4.0 Å off the left lead where the larger absorption distance makes a slightly larger total energy by less than 100 meV. The surface magnetic moment at the Fe or molecule contact is more stable when bond length is varied around 4.0 Å. We therefore fixed the contact distance to be 4.0 Å throughout the calculations.

[18] J. Taylor, H. Guo, and J. Wang, Phys. Rev. B **63**, 245407 (2001); **63**, 121104 (2001).

[19] In NEGF-DFT calculation, the Hamiltonian is converged to 1.0^{-4} eV. We use a double zeta polarized linear combination of atomic orbitals (LCAO) basis and the exchange correlation is treated at the local spin-density approximation level. As a check to the basis, we confirmed that electronic structures of bulk Fe as well as gas phase molecules N_2, CH_4, and H_2 all well reproduce those obtained from the full potential linearized augmented plane-wave (LAPW) method.

[20] S. Ohnishi, A. J. Freeman, and M. Weinert, Phys. Rev. B **28**, 6741 (1983).

[21] C. C. Kaun and Hong Guo, Nano Lett. **3**, 1521 (2003).

[22] S. S. P. Parkin, C. Kaiser, A. Panchula, P. M. Rice, B. Hughes, M. Samant, and S. H. Yang, Nature Mater. **3**, 862 (2004); S. Yuasa, T. Nagahama, A. Fukushima, Y. Suzuki, and K. Ando, *ibid.* **3**, 868 (2004).